



Theoretical studies on the reaction mechanism of $\text{CF}_3\text{CF}=\text{CF}_2$ with OH



Li-ling Ai, Xue-mei Duan, Jing-yao Liu*

Institute of Theoretical Chemistry, State Key Laboratory of Theoretical and Computational Chemistry, Jilin University, Changchun 130023, People's Republic of China

ARTICLE INFO

Article history:

Received 10 January 2013
 Received in revised form 22 February 2013
 Accepted 25 February 2013
 Available online 7 March 2013

Keywords:

$\text{CF}_3\text{CF}=\text{CF}_2$
 OH radicals
 Density functional theory
 MCG3/3
 Reaction mechanism

ABSTRACT

Quantum mechanical calculations have been performed at the MCG3//M06-2X/aug-cc-pVDZ level to explore the OH-initiated oxidation of $\text{CF}_3\text{CF}=\text{CF}_2$. The calculated results show that the $\text{CF}_3\text{CF}=\text{CF}_2 + \text{OH}$ reaction occurs via addition–elimination mechanism, leading to products $\text{CF}_3\text{CFCF}(\text{O})$, $\text{CF}_3\text{C}(\text{O})\text{CF}_2$ and HF. In the presence of O_2/NO , the primary products are $\text{CF}_3\text{C}(\text{O})\text{F}$ and $\text{CF}_2(\text{O})$, in good agreement with the experimental observations.

© 2013 Elsevier B.V. All rights reserved.

1. Introduction

Chlorofluorocarbons (CFCs) from industrial applications have been phased out due to their well-known connection with global warming [1,2] and detrimental effect on the stratospheric ozone layer [3–6]. An international effort has been made to replace these ozone-depleting chemicals with more environmentally friendly alternatives. Fluorinated alkenes, which contain no Cl atoms and do not contribute to the ozone depletion, are currently being considered as an important class of potential substitutes for CFCs and widely used in chemical industry as starting materials in syntheses of various halogenated compounds and in fluoropolymer production. However, they may still potentially cause the global warming effect due to containing numerous C–F bonds. Fluorinated alkenes may react with NO_3 , O_3 and $\text{O}(^3\text{P})$ in the atmosphere [7–12], but the reaction with the OH radicals is known to be the primary atmospheric degradation process under atmospheric condition. They are susceptible to attack by OH, due to containing C=C bond(s) [13]. To assess its environmental impact and to estimate the atmospheric lifetime, the removal process by OH has attracted much attention [14–16].

In this work, we focus on the perfluoropropylene molecule, $\text{CF}_3\text{CF}=\text{CF}_2$. Considerable experimental investigations on the kinetics of $\text{CF}_3\text{CF}=\text{CF}_2 + \text{OH}$ reaction have been reported [8,9,17–21]. $\text{CF}_3\text{C}(\text{O})\text{F}$ and $\text{CF}_2(\text{O})$ were proposed as the dominant products for the OH-initiated oxidation of $\text{CF}_3\text{CF}=\text{CF}_2$ in the presence of O_2 and NO. However, the detailed mechanism for this process is still

elusive. There are some computational studies [10,22,23] of $\text{CF}_3\text{CF}=\text{CF}_2$, however, to the best of our knowledge, no theoretical attention has been paid to the $\text{CF}_3\text{CF}=\text{CF}_2 + \text{OH}$ reaction. In view of its potential importance, herein, we carried out density functional electronic structure calculations of the most relevant stationary points and reaction pathways on the potential energy surfaces (PESs) for the $\text{CF}_3\text{CF}=\text{CF}_2 + \text{OH}$ reaction in the absence and presence of O_2/NO . The main objectives of the present paper are to provide a comprehensive understanding for the chemical transformation processes of $\text{CF}_3\text{CF}=\text{CF}_2$ initiated by OH oxidation, and give the primary oxidation product information under atmospheric condition. The comparison between theoretical and experimental studies is made. The present results are helpful for better evaluating the environmental impact of $\text{CF}_3\text{CF}=\text{CF}_2$.

2. Calculation methods

All of the electronic structure calculations were carried out using the GAUSSIAN 09 suit of programs [24]. The optimized geometries of all the stationary points (including reactants, complexes, transition states, intermediates, and products) were obtained by the M06-2X density functional method [25] with the aug-cc-pVDZ [26,27] basis set (M06-2X/aug-cc-pVDZ). The nature of each critical point is characterized by harmonic vibrational frequency analysis, that is, all of the minimum possess only real frequencies, whereas the transition states possess one and only one imaginary frequency. To obtain zero-point energy (ZPE) corrections, a factor of 0.9721 [25] is used to scale the M06-2X/aug-cc-pVDZ frequencies. In addition, the minimum-energy path (MEP) was calculated by the intrinsic reaction coordinate (IRC)

* Corresponding author. Fax: +86 431 88498026.

E-mail addresses: ljl121@jlu.edu.cn, jingyao121@gmail.com (J.-y. Liu).

theory [28,29] to confirm that the transition states connect designated isomers or products. To obtain more reliable energetics, the higher-level single-point calculations were performed by the multi-coefficient Gaussian-3/version-3 (MCG3/3) method [30–32] based on the M06-2X/aug-cc-pVDZ optimized geometries. The MCG3 calculations were carried out by using the MLGAUSS program version 2.0 [33] in conjunction with the GAUSSIAN 03 program packages [34].

3. Results and discussion

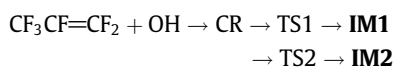
There are two conformers of the reactant $\text{CF}_3\text{CF}=\text{CF}_2$. Since the energy difference between them is 1.4 kcal/mol at the M06-2X/aug-cc-pVDZ level. Thus, in the following study, only the stable conformer is taken into account.

3.1. Addition–elimination mechanism

The optimized geometries of the most important reactants, complexes, transition states, intermediates and products involved in the addition–elimination processes are presented in Fig. 1 along with the available experimental data [35]. The other geometric data are summarized in Table S1 (see Supporting information). The energetic data of all stationary points at the M06-2X/aug-cc-pVDZ and MCG3//M06-2X/aug-cc-pVDZ levels are listed in Table S2. The vibrational frequencies of all stationary points are shown in Table S3. The schematic PESs obtained at the MCG3//M06-2X/aug-cc-pVDZ level are depicted in Fig. 2a and b. For convenient discussion, the total energy of the reactant $\text{R CF}_3\text{CF}=\text{CF}_2 + \text{OH}$ is set to be zero for reference.

3.1.1. Entrance channels

The reaction of OH radical with $\text{CF}_3\text{CF}=\text{CF}_2$ proceeds via electrophilic addition of OH radical to the unsaturated >C=C< double bond of $\text{CF}_3\text{CF}=\text{CF}_2$. A pre-reactive van der Waals complex CR is located at the entrance channel at the M06-2X/aug-cc-pVDZ level, where the C1–O10 and C2–O10 bond lengths are 2.61 and 2.72 Å, respectively. CR lies 1.8 kcal/mol below the reactants. Starting from CR, two addition pathways are found, i.e., addition to either terminal carbon atom to form intermediate **IM1** $\text{CF}_3\text{CFCF}_2(\text{OH})$ via TS1 or central carbon atom to form intermediate **IM2** $\text{CF}_3\text{CF}(\text{OH})\text{CF}_2$ via TS2.



Seen from Fig. 2a and b, TS1 and TS2 lie 2.3 and 1.7 kcal/mol below the separate reactants, respectively, and the two addition processes are highly exothermic by 47.9 and 44.4 kcal/mol, respectively, which means that both addition processes almost do not need to overcome potential barriers, and thus are kinetically and thermodynamically favorable. Note that CR lies higher than TS1 by 0.5 kcal/mol after high-level single-point energy calculation at the MCG3//M06-2X/aug-cc-pVDZ level. To further testify the accuracy and reliability of this value, the high-level single-point energy calculations are also done at the BMC-CCSD//M06-2X/aug-cc-pVDZ and G3(MP2)//M06-2X/aug-cc-pVDZ levels. It is shown that CR is higher than TS1 by 0.9 and 0.78 kcal/mol, respectively, at the two levels, which are very close to the value obtained at the MCG3//M06-2X/aug-cc-pVDZ level. The BMC-CCSD and G3(MP2) energies are given in Table S4. The addition process makes intermediates **IM1** and **IM2** are highly activated, so further isomerization or dissociation are considered below.

3.1.2. Isomerization and dissociation of **IM1** and **IM2**

As shown in Scheme 1 and Fig. 2a, starting from the most favorable entrance intermediate **IM1** $\text{CF}_3\text{CFCF}_2(\text{OH})$ (–47.9 kcal/mol), seven production channels are identified. Firstly, **IM1** can undergo a H-migration from the OH group to the central-C to form **IM3** $\text{CF}_3\text{CHF}(\text{O})\text{CF}_2$ (–35.5 kcal/mol) via a four-membered ring transition state TS3 (barrier height of 37.0 kcal/mol). Subsequently, by breaking the C–C bonds, **IM3** can either give rise to **P1** $\text{CF}_3\text{CHF} + \text{CF}_2(\text{O})$ (–44.3 kcal/mol) via TS4 or dissociate to **P2** $\text{CF}_3 + \text{CHF}(\text{O})\text{CF}_2$ (–7.0 kcal/mol) without an exist barrier. The energy barrier from **IM3** to **P1** for path1 is only 4.8 kcal/mol, and thus path1 is more favorable than path2.

Secondly, **IM1** can isomerize to **IM4** $\text{CF}_3\text{CF}_2\text{CF}(\text{OH})$ (–46.5 kcal/mol) via a three-center transition state TS5. This step requires surmounting a barrier height of 33.8 kcal/mol. Starting from **IM4**, four possible reaction paths have been found. Path3 is the formation of **P3** $\text{CF}_3\text{CFCF}(\text{O}) + \text{HF}$ (–54.9 kcal/mol) via a five-membered ring transition state TS6. This process needs to overcome a barrier of 28.7 kcal/mol. Path4 is the H-extrusion of the O–H bond to form **P4** $\text{CF}_3\text{CF}_2\text{CF}(\text{O}) + \text{H}$ (–26.9 kcal/mol) via TS7 with a barrier of 32.9 kcal/mol. Path5 and path6 present the C–C bond ruptures to produce **P5** $\text{CF}_3 + \text{CF}_2\text{CF}(\text{OH})$ (–3.42 kcal/mol) via TS8 (–3.39 kcal/mol) and **P6** $\text{CF}_3\text{CF}_2 + \text{CF}(\text{OH})$ (3.9 kcal/mol) with no distinct barrier, respectively. Since the transition states or fragment products in the latter three pathways paths 4–6 lie higher than the former, path3 giving **P3** is the most feasible channel from **IM4**.

Thirdly, **IM1** is easily isomerized to another rotation isomer **IM1A** (–48.2 kcal/mol) via TS9 by rotation of the C–O bond, by overcoming a small barrier of 1.0 kcal/mol. One dissociation channel from **IM1A** (path7) undergoes a 1,4-HF-elimination to form **P7** $\text{CF}_2=\text{CFCF}_2(\text{O}) + \text{HF}$ (–11.3 kcal/mol) via a six-membered ring transition state TS10, with a large energy barrier of 41.4 kcal/mol relative to **IM1A**, and thus is unimportant.

Among these seven pathways from **IM1**, it is seen that the transition state TS6 (–17.8 kcal/mol) in path3 lies much lower than the rate-determining transition states in the other paths. Thus, path3 giving **P3** is energetically most favorable.

Starting from intermediate **IM2** $\text{CF}_3\text{CF}(\text{OH})\text{CF}_2$ (–44.4 kcal/mol), there are five possible reaction pathways as exhibited in Scheme 1 and Fig. 2b. **IM2** can isomerize to intermediate **IM5** $\text{CF}_3\text{CF}(\text{O})\text{CHF}_2$ (–36.2 kcal/mol) via a four-membered ring transition state TS11 (–5.0 kcal/mol). A barrier of 39.4 kcal/mol must be traversed for this process. Once formed, by the scissions of the two different C–C bonds, **IM5** can decompose to produce **P8** $\text{CF}_3\text{CF}(\text{O}) + \text{CHF}_2$ (–35.4 kcal/mol) through TS12 and **P9** $\text{CF}_3 + \text{CF}(\text{O})\text{CHF}_2$ (–33.3 kcal/mol) through TS13. The barrier heights are 6.1 and 9.8 kcal/mol for these two processes, respectively. Apparently, due to the higher-lying rate-determining transition state TS11, the formation of two dissociation products **P8** and **P9** are kinetically unfeasible.

Intermediate **IM6** $\text{CF}_3\text{C}(\text{OH})\text{CF}_3$ (–56.9 kcal/mol) can be formed through the migration of F atom to the terminal-C in **IM2** via a three-center transition state TS14 (–12.5 kcal/mol). Also, **IM2** interconverts to **IM2A** (–44.6 kcal/mol) via a C–O bond rotation transition state TS15 (–41.5 kcal/mol), followed by isomerization to **IM6** via TS16 (–12.0 kcal/mol). Starting from **IM6**, three reaction paths have been found. Path10 exhibits the formation of **P10** $\text{CF}_3\text{C}(\text{O})\text{CF}_3 + \text{H}$ (–20.8 kcal/mol) via a O–H cleavage transition state TS17. This step is unfavorable due to a higher barrier, up to 44.8 kcal/mol. Path11 gives a description of 1,4-HF-elimination from **IM6** via a five-membered ring transition state TS18, resulting in the formation of **P11** $\text{CF}_3\text{C}(\text{O})\text{CF}_2 + \text{HF}$ (–46.3 kcal/mol). This process is energy-demanding with a barrier height of 37.7 kcal/mol with respect to **IM6**. **IM6** can also undergo direct C–C bond cleavage to give **P12** $\text{CF}_3\text{C}(\text{OH}) + \text{CF}_3$ without an exist barrier.

Download English Version:

<https://daneshyari.com/en/article/5394177>

Download Persian Version:

<https://daneshyari.com/article/5394177>

[Daneshyari.com](https://daneshyari.com)